

# Nonlinear dynamics of vortexlike domain walls in magnetic films with in-plane anisotropy in a pulsed magnetic field

B. N. Filippov, L. G. Korzunin, and F. A. Kassan-Ogly

*Institute of Metal Physics, Ural Division, Russian Academy of Sciences, ul. S. Kovalevskoi 18, Ekaterinburg 620219, Russia*

(Received 21 November 2003; revised manuscript received 28 April 2004; published 11 November 2004)

The nonlinear dynamic behavior of domain walls with a vortexlike internal structure moving under the action of a pulsed magnetic field in magnetic films having an in-plane anisotropy was investigated by numerical solving the Landau-Lifshitz equations. In the framework of a two-dimensional model, the main interactions, including a dipole-dipole one (in the continuum approximation), are explicitly taken into account. Isolated and periodic field pulses with arbitrary amplitude and duration are considered. A possibility of transitions between various stationary states of wall motion induced by the pulsed fields is predicted. The transitions are shown to occur by the complicated nonlinear rearrangement of the wall structure. There are two distinctive intervals of pulse duration in which the nonlinear dynamic rearrangement radically differ. The film thickness and the magnitude of saturation induction are the main factors that have an influence on the transitions between stationary states. The periodic field pulses are established to govern the regime of wall motion, in particular, to alter the period of dynamic structure rearrangement of walls moving in a constant magnetic field. Moreover, the periodic field pulses may either completely suppress the nonstationary motion or, on the contrary, promote its development in the propulsive fields below some critical value.

DOI: 10.1103/PhysRevB.70.174411

PACS number(s): 75.70.Kw, 05.45.-a, 87.17.Aa

## I. INTRODUCTION

Domain walls are nonlinear objects localized in space (on the order of hundreds of nm) that separate adjacent uniformly magnetized regions (domains). In magnetic films walls have a much more complicated internal structure (see, for example, Refs. 1 and 2) than initially assumed.<sup>3</sup> In the presence of an external magnetic field directed along the magnetization of one of the domains the walls not only move but also change their internal structure. These changes may be of a global nonlinear character. They are topological solitons having internal degrees of freedom. We believe that the study of such nonlinear objects is of essential importance for nonlinear physics. A wall is an array of elementary magnetic moments, each of which behaves as an isolated gyroscope. Walls not only move in response to external fields, but also show inertial properties, the gyroscopic properties of elementary moments leading to several peculiarities, such as the appearance of wall retrograde motion.<sup>4</sup>

Wall dynamics is also important for applications, in particular, for the electromagnetic loss and magnetic noise, for optimization of the high-frequency information read-out, and estimation of the time of pulsed magnetization reversal of films, etc. The estimation of properties on the assumption of the Bloch character of walls can lead to substantial errors.<sup>5</sup> The nonlinear dynamics of domain walls in magneto-ordered materials has many branches. Walls exist in ferromagnetic and antiferromagnetic substances, as well as in the materials with other types of magnetic ordering. They exist in bulk specimens, small particles, and thin films. There is a wide variety of wall structure peculiarities in single-crystal films with different types of anisotropy, as well as in magnetic uniaxial films with a perpendicular and an in-plane anisotropy. Along with the general laws, specialized methods are required in each case. We confine ourselves to the study of

the wall nonlinear dynamics in magnetic films with in-plane anisotropy.

In view of development efforts of the miniature inertialess and energy-free memory in magnetic films with a large perpendicular anisotropy (quality factor  $Q > 1$ ,  $Q = K/2\pi M_s^2$ ,  $K$  is the constant of uniaxial anisotropy and  $M_s$  is the saturation magnetization), a considerable understanding of nonlinear dynamic behavior of such films has been obtained.<sup>1</sup> For films with an in-plane anisotropy and low quality factor ( $Q < 1$ ), important achievements in nonlinear wall behavior were reached during the last decade. Such films are also used in the information read-out heads (see, for example, Refs. 6–8). Some lag in the studies of nonlinear dynamics of walls in these films is related to the important role of dipole-dipole interaction that is difficult to explicitly take into account due to its long-range character. However, the internal structure of the walls appears to be the most interesting.

The internal structure of a wall is asymmetric and vortexlike as was initially shown by LaBonte<sup>9</sup> (see also Ref. 10). Such a structure was obtained by the numerical minimization of the full energy functional, in which within the framework of a two-dimensional magnetization distribution all the main types of interaction—an inhomogeneous exchange, a magnetic anisotropy, and a dipole-dipole one (in the continuum approximation)—were taken into account for the first time. The asymmetric vortexlike structure of the walls seems to be universal existing in the films in a wide range of their thickness, since such a structure allows for more complete magnetic flux closure in the films than other structures. Only in films with small thickness (less than 40 nm in Permalloy films) the Néel wall becomes more favorable. This is valid only in the absence of a surface anisotropy.<sup>11</sup> Similar asymmetric vortexlike walls exist in single-crystal films with a cubic symmetry.<sup>12</sup> There are a series of papers in which the existence of asymmetric vortexlike walls is supported experimentally.<sup>12–16</sup>

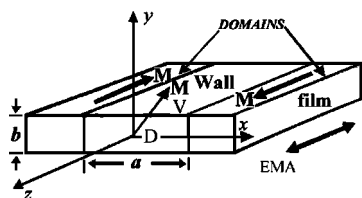


FIG. 1. Geometry of the problem.

The pioneer studies of dynamic properties of the walls with a vortexlike structure are described in Ref. 2. In our opinion, Yuan and Bertram<sup>5</sup> have advanced this, demonstrating that the effective mass of a wall with a vortex structure may exceed the mass of a one-dimensional Bloch wall by two orders of magnitude. Moreover, they showed that at the nonstationary motion of walls (in the fields above some critical value  $H_c$ ) the nonlinear rearrangements in their internal structure occur.

In a series of papers, we demonstrated a strong influence of a surface anisotropy on the nonlinear dynamics of vortexlike walls,<sup>17</sup> predicting subperiodic velocity oscillations in the fields above  $H_c$ ,<sup>18</sup> revealed a nonmonotonic dependence of a critical field  $H_c$  on a film thickness and the saturation induction,<sup>19,20</sup> etc. All these results were obtained for the case of walls moving under the action of a constant magnetic field  $\mathbf{H}$ . More generally (for example, in the studies of pulsed magnetization reversal processes of magnetic films) the knowledge of a wall dynamic behavior in pulsed magnetic fields is required. At present there are no papers on the dynamic behavior of asymmetric vortexlike walls under the action of a pulsed magnetic field. Current studies in constant fields reveal that the process of dynamic rearrangement of a wall structure occurs nonuniformly in time, such that some transient wall configurations have greater lifetimes than the others. As a consequence, there is no need to supply a constant field, but it is sufficient to switch on a single pulse of a magnetic field of a particular duration. Such magnetic field pulses may be used to induce transitions between different stationary wall configurations (in the fields below  $H_c$ ).

This paper is devoted to such nonlinear phenomena. It will be shown, in particular, that with a choice of pulse parameters one can either vary the period of dynamic rearrangements in the internal structure of domain walls or completely suppress their nonstationary motion.

## II. STATEMENT OF THE PROBLEM AND BASIC EQUATIONS

We consider a uniaxial magnetic film of thickness  $b$  with a surface parallel to the  $xz$  plane and an easy axis directed along the  $z$  axis (see Fig. 1).

The magnetic state of the film corresponds to two domains with uniform saturation magnetization  $\pm M_s$ , oriented along  $+z(-z)$  at  $x > a/2(x < -a/2)$ . We assume that a domain wall is entirely located in a region  $V$  with a rectangular cross-section  $D$  in the  $xy$  plane and a length  $a$  along the  $x$  axis. The magnetization configuration is assumed two-dimensional ( $\mathbf{M} = \mathbf{M}(x, y)$ ) in the region  $D$ . The equilibrium configurations corresponding to minimal energy  $E$  can be found by

numerical minimization of the functional (per unit length along the  $z$  axis)

$$E = \int_D \int \left\{ A \left[ \left( \frac{\partial \mathbf{m}}{\partial x} \right)^2 + \left( \frac{\partial \mathbf{m}}{\partial y} \right)^2 \right] - K(\mathbf{m} \cdot \mathbf{c})^2 - \frac{1}{2} M_s (\mathbf{m} \cdot \mathbf{H}^{(m)}) \right\} dx dy. \quad (1)$$

Here the first, second, and third terms are the density of the exchange, magnetic anisotropy, and dipole-dipole (in the continuum approximation) energies;  $A$  is the exchange parameter,  $\mathbf{c}$  is the unit vector along an easy axis,  $\mathbf{m} = \mathbf{M}/M_s$ ,  $\mathbf{H}^{(m)}$  is a magnetostatic field determined by magnetostatic equations with the usual boundary conditions. For solving the problem we use the constancy of the magnetization absolute value and the following boundary conditions:

$$\left[ \mathbf{m} \times \frac{\partial \mathbf{m}}{\partial y} \right] \Big|_{y=\pm b/2} = 0; \quad (2)$$

$$m_z|_{x=\pm a/2} = \pm 1, \quad m_x|_{x=\pm a/2} = 0, \quad m_y|_{x=\pm a/2} = 0. \quad (3)$$

For numerical minimization of the functional (1) we followed the method developed by LaBonte.<sup>9</sup> According to it, a rectangular grid divides the region  $D$  into small cells. The region  $V$  is divided into parallelepipeds stretched along the  $z$  axis, whose sidewalls are parallel to the coordinate planes  $xz$  and  $yz$ . The cells are assumed to have macroscopic, but so small, sizes that in every point of each of these parallelepipeds the  $\mathbf{m}$  direction may be considered to be uniform. Along the  $z$  direction  $\mathbf{m} = \text{const}$ . The  $\mathbf{m}$  orientation in  $D$  varies from cell to cell. One can find the details in Refs. 18 and 20.

The numerical calculations were carried out on the grids with various numbers of cells and various  $a/b$  ratios. The maximum mesh of the grid was  $90 \times 30$ . The greater number of cells significantly increases the computation time, but only slightly changes the numerical results. The  $a/b$  ratio varied in the range  $1 \leq a/b \leq 6$ . We used the magnitudes  $A = 10^{-6}$  erg/cm,  $K = 10^3$  erg/cm<sup>3</sup>, and  $M_s = 800$  emu cm<sup>-3</sup>, which are characteristic of Permalloy films, as the basal parameters of the film. For the end of the computations, we utilized the widely used criterion<sup>5,9,11</sup> proposed by Aharoni.<sup>21</sup> Figure 2 shows the  $\mathbf{m}$  distributions in the  $xy$  plane that is perpendicular to the film surface and to easy axis.

Walls with these  $\mathbf{M}$  configurations in the  $xy$  plane are the asymmetric Bloch walls of LaBonte<sup>9</sup> and Hubert<sup>10</sup>. The  $\mathbf{m}$  projection is seen to vary from domain to domain in such a way that a magnetization vortex appears. Upon the transition from one domain to the other the  $z$  component of  $\mathbf{m}$  varies as well. The central dashed line in the figure [ $y = y_0(x)$ ] corresponds to a zero value of  $m_z$  (the wall center) and is asymmetric with respect to the  $y$  axis. Two other lines of the  $m_z = \text{const}$  level are drawn such that between them the  $\mathbf{m}$  direction varies by about  $60^\circ$ . We designate a wall right asymmetric, if its vortex center is located to the right from the central line and left asymmetric otherwise. The walls in Figs. 2(a) and 2(b) are left asymmetric and in Figs. 2(c) and 2(d) right asymmetric. The walls may have different chirality (a different direction of the magnetization curling in a vortex).

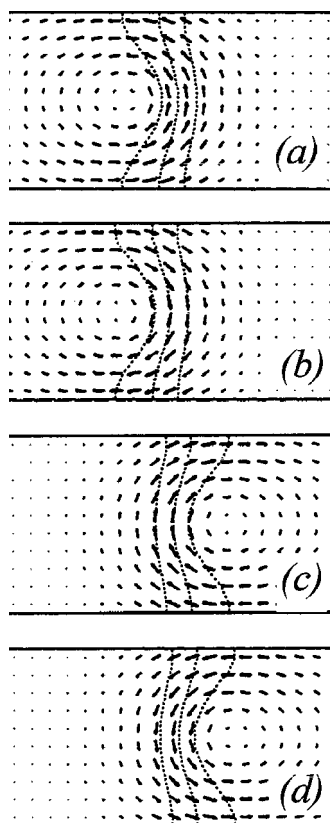


FIG. 2. Possible static configurations of the magnetization in asymmetric domain walls, having the same energy; (a) and (d) differ from (b) and (c) by chirality. Films with basal parameters,  $b=50$  nm.

All four walls have the same energy, so we have four-fold degeneracy over the magnetization configurations (two-fold over chirality and two-fold over a symmetry type). The structures shown in Fig. 2 are stable in a wide range of magnetic parameters and film thickness. Our studies revealed the existence of the other two-dimensional wall structures, but they turn out to be metastable, except for the special cases (see Ref. 11). Asymmetric structures with two walls are considered in Refs. 22 and 23.

The study of nonlinear dynamics of the domain walls described was done by a direct numerical solution of the Landau-Lifshitz equation,<sup>24</sup> written in dimensionless form:

$$(1 + \alpha^2) \frac{\partial \mathbf{m}}{\partial \tau} = -[\mathbf{m} \times \mathbf{h}_{eff}] - \alpha[\mathbf{m} \times [\mathbf{m} \times \mathbf{h}_{eff}]], \quad (4)$$

where  $\tau = \gamma M_s t$ ,  $t$  is real time,  $\gamma$  is the gyromagnetic ratio,  $\alpha$  is a dimensionless Gilbert damping parameter related to the isotropic local damping parameter  $\lambda$  introduced by Landau and Lifshitz<sup>24</sup> by the relation  $\alpha = \lambda / |\gamma| M_s$ ,  $\mathbf{h}_{eff}$  is a dimensionless effective field in which the magnetization moves:

$$\mathbf{h}_{eff} = \mathbf{h}_e + \mathbf{h}^{(m)} - k_A (\mathbf{m} \cdot \mathbf{c}) \mathbf{c} + \mathbf{h}, \quad (5)$$

where

$$\mathbf{h}_e = \frac{\partial^2 \mathbf{m}}{\partial \xi^2} + \frac{\partial^2 \mathbf{m}}{\partial \eta^2},$$

$$\mathbf{h}^{(m)} = \mathbf{H}^{(m)} / M_s, \quad \mathbf{h} = \mathbf{H} / M_s,$$

$$k_A = 2K / M_s, \quad \xi = x / b_0,$$

$$\eta = y / b_0, \quad b_0 = \sqrt{A / M_s}. \quad (6)$$

To numerically calculate the expression (4) with boundary conditions (2) and (3) we use the same spatial grid as upon the minimization of the functional  $E$ . We also use the predictor-corrector method (see Ref. 25). The distribution  $\mathbf{m}_0$  (i.e.,  $\mathbf{m}$  in each cell of the spatial grid) is initialized at the moment  $\tau=0$ . The  $\mathbf{m}_0$  configuration is determined by numerical minimization of the functional (1). In the first step (predictor) an iteration  $\mathbf{m}_{n+1}$  is determined by the formula

$$\mathbf{m}_{n+1}^* = \mathbf{m}_n + \Delta \tau \mathbf{f}(\tau_n, \mathbf{m}_n), \quad (7)$$

where

$$\begin{aligned} \mathbf{f}(\tau_n, \mathbf{m}_n) = & -\frac{1}{1 + \alpha^2} ([\mathbf{m}_n \times \mathbf{h}_{eff}(\mathbf{m}_n)] \\ & + \alpha [\mathbf{m}_n \times [\mathbf{m}_n \times \mathbf{h}_{eff}(\mathbf{m}_n)]]). \end{aligned} \quad (8)$$

In the second step (corrector) the iteration  $\mathbf{m}_{n+1}$  is finally determined:

$$\mathbf{m}_{n+1} = \mathbf{m}_n + \Delta \tau \mathbf{f}(\tau_n, \mathbf{m}_{n+1}^*). \quad (9)$$

The time step  $\Delta \tau$  is variable, being chosen such that the maximal rotation angle of the magnetization vector in a cell is less than a given value.

We used random perturbations of arbitrary amplitude at an arbitrary time and arbitrary initial  $\mathbf{M}$  configurations to evaluate the stability of the solutions. A shift of the computation region was used to keep the wall centered to the line ( $m_z=0$ ). On this line, the quantity  $m_x^4 + m_y^4$  acquires its maximum value and it is just the quantity that is computed for wall shifting. The static solutions described previously are obtained quickly and used as initial conditions for the dynamic solutions.

### III. RESULTS AND DISCUSSION

#### A. General results

The structure of a wall changes with time under the action of either constant or pulsed magnetic fields and a large number of various instantaneous wall configurations appear upon its motion. Some of them are retained after switching off external fields, for example, those shown in Fig. 2. They are stable, but there also exist metastable configurations (see below). Such configurations may alter in the presence of external fields.

A certain critical field  $H_c$  (bifurcation field) was shown to exist, below (above) which the walls with a two-dimensional  $\mathbf{M}$  distribution move stationary (nonstationary).<sup>4,5</sup> In particular, for fields slightly higher than  $H_c$ , the wall internal structure and velocity vary periodically<sup>4,5</sup> with a period  $T$ . The period strongly depends on the total field directed along easy axis. If a wall has one of configurations shown in Fig. 2, then some transient process occurs after applying the field  $H < H_c$

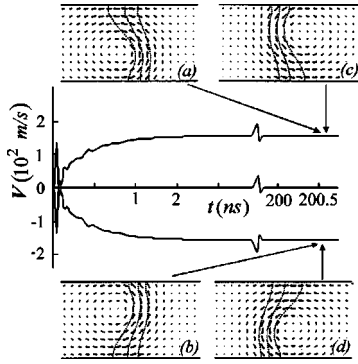


FIG. 3. Time dependence of the velocity of walls with different chiralities. A transition to the stationary motion is shown for films with basal parameters,  $b=50$  nm,  $H=90$  Oe, and  $\alpha=0.1$ .

along the  $z$  axis. During this process an intrawall vortex begins to shift to one of the film surfaces: to the lower (upper) surface on the left-side (right-side) wall, which is shown in Fig. 3 for two opposite directions of the constant external field. This effect of vortex shifting was described in Refs. 5, 10, and 15 and is related to the gyrocoupling force.<sup>26</sup> The vortex center localizes at some distance from a film surface, and then the walls with such configurations move stationary. The wall structure and velocity do not change upon stationary motion in a constant field, and such  $\mathbf{M}$  configurations that are formed after all transient processes are called steady state. Apart from the configurations shown in Fig. 3 one more configuration, namely, the Néel wall (see below and Ref. 10) is also steady state, but it is metastable at  $H=0$ .

All the other configurations are merely intermediate (instantaneous states) that appear during nonstationary wall motion and disappear upon stationary motion and after switching off the fields. It should be noted, however, that any solution, including intermediate, is stable. In other words, given the same parameters in every repeated numerical experiment a wall undergoes the same sequence of intermediate states. Moreover, we used random perturbations of arbitrary amplitude at an arbitrary time to estimate the stability of interwall transformation sequences during long time intervals. We consider the dynamic behavior of domain walls subjected to either isolated or periodically repeated pulses of magnetic field  $H_i$  directed along an easy axis (the  $z$  axis). The pulsed field is either added to constant magnetic field  $H$  also directed along the  $z$  axis, or the constant field may be zero. Although data presented is for rectangular-shaped pulses, the main conclusions are also valid for smoothed pulses. The wall behavior is different when the total applied field  $H_t=H+H_i$  is below or above the critical field  $H_c$  even if  $H < H_c$ . The most interesting situations we consider occur when (1)  $H < H_c < H_t$ , and (2)  $H > H_c$ .

As was shown in Refs. 5 and 18, the character of the dynamic rearrangement of a wall structure under the action of an external field applied along an easy axis and exceeding the critical field  $H_c$  varies with varying film thickness within quite a narrow thickness range about some critical value  $b_c$ . We will call films relatively thin if  $b < b_c$  and relatively thick otherwise. Permalloy films are relatively thin for  $b < 65$  nm, where the dynamic rearrangement of a wall structure has a

classical character<sup>5</sup> and the thickness dependence of  $H_c$  is almost linear.<sup>19</sup> Permalloy films with  $b > 65$  nm, whose character of dynamic rearrangement of a wall structure substantially differs from classical behavior, are relatively thick.

## B. Interwall transitions induced by isolated pulses

If an additional pulsed magnetic field  $H_i$  is applied to a wall with a certain magnetization configuration moving in a constant field, then its configuration and velocity change. It seems natural that the wall structure and velocity should relax to the initial state after switching off the pulsed field. However, as our numerical experiment show, the situation is more complicated, and the results substantially depend on the duration of applied pulse at  $H+H_i > H_c$ . Three different pulse duration ranges can be discriminated: (1)  $0 < \Delta t < \Delta t_m$ , (2)  $\Delta t_m < \Delta t < \Delta t_M$ , and (3)  $\Delta t_M < \Delta t < \Delta t_m + T/2$ , resulting in quite different final steady states after the nonlinear dynamic rearrangement of a wall internal structure. Here  $\Delta t_m$  is the minimum pulse duration, beginning with which the rearrangement of a steady state configuration (existing in the field  $H$ ) occurs.  $\Delta t_M$  is the minimum pulse duration, after switching off of which a steady state of  $3a$  type (but with an opposite chirality) is formed.  $T$  is the period of the wall structure dynamic rearrangement at  $H > H_c$  (see Sec. III A).

### 1. Interwall transitions in relatively thin films

In a trivial (1) case, when  $\Delta t < \Delta t_m$ , the wall structure and velocity actually relax to the initial state. More interesting results are obtained in (2)  $\Delta t_m < \Delta t < \Delta t_M$  and (3)  $\Delta t_M < \Delta t < \Delta t_m + T/2$  cases that will be called the short and long pulse duration range, respectively. We studied the wall velocity and dynamic behavior for a wide set of parameters and pulse durations. Figures 4 and 5 show typical changes of the wall velocity averaged over the film thickness and instantaneous magnetization configurations for two different pulse durations  $\Delta t_1 \in (\Delta t_m, \Delta t_M)$  and  $\Delta t_2 \in (\Delta t_M, \Delta t_m + T/2)$ .

A constant magnetic field  $H=90$  Oe along the  $z$  axis is switched on at  $t=0$ . Then initial 4(a) and 5(a) wall structures rearrange to the steady state moving 4(b) and 5(b) structures, after which field pulses of various durations are triggered. The letters **I** and **O** denote the switching on and switching off of a pulse, respectively. It seems natural that the wall structure should relax to the initial steady states (shown in Figs. 4 and 5) after switching off the pulsed field, but, given  $H$ ,  $H_c$ , and pulse durations, the other physical phenomena occur. First, the character of transition to a new steady state of the wall motion after switching off of the pulse substantially depends on its duration, second, the final state (magnetization distribution after transient process termination) also depends on the pulse duration. Thus, transitions between different steady states occur by the nonlinear dynamic rearrangement of the wall internal structure. The 4(a) and 5(a) steady states with a velocity of  $\sim 155$  m/s are established in  $\sim 2$  ns. After that, pulsed field  $H_i$  may be triggered at an arbitrary time instant  $t_0$ , and the result does not depend on the instant. The data in Figs. 4 and 5 refer to  $t_0=110$  ns and  $H_i=15$  Oe.

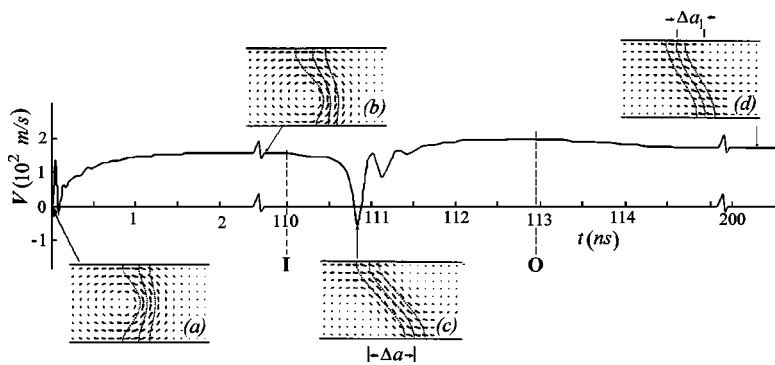


FIG. 4. Time dependence of the velocity of walls in a constant field  $H=90$  Oe and pulsed field  $H_i=15$  Oe, 50 nm thickness,  $\alpha=0.1$ . Instantaneous wall configurations (a)–(d) illustrate the rearrangement of a wall during its motion. The pulse beginning and ending times are denoted in the figures by the letters **I** and **O**, respectively. The pulse duration is  $\Delta t=0.64$  ns.

**2. Interwall transitions for short range of pulse duration**

In this case, the pulse duration was chosen to be  $\Delta t_1=0.64$  ns. After switching off the pulse the vortex continues to shift to the lower film surface, and finally the wall begins to rearrange to the asymmetric Néel wall [Fig. 4(c)], its velocity begins to decrease. Then at some time instant the pulse is switched off, but the rearrangement continues. In particular, the wall in Fig. 4 transforms to the asymmetric Néel wall with a structure depicted in Fig. 4(c), its velocity is minimal and the span  $\Delta a$  of the central line (the distance between projections of end points onto a film surface) maximal. Thus a new steady state of a wall is gradually established with a 4(d) structure ( $\Delta a_1 < \Delta a$ ) and with a velocity that differs from the velocity of a wall with a 4(b) structure, or, in other words, a 4(b)  $\rightarrow$  4(d) transition occurs. The same transitions occur for all  $\Delta t_1 \in (\Delta t_m, \Delta t_M)$ . Note that if  $H_i$  is sufficiently high (comparable to  $H$ ), then  $\Delta t_m$  can be estimated by the time of a 4(c) structure appearance.

**3. Interwall transitions for long range of pulse duration**

If after establishing the steady state motion with the 5(c) structure a pulse of the field  $H_i=15$  Oe and  $\Delta t_2=2.9$  ns duration is switched on, then dynamic rearrangement of the structure occurs differently. In this case, after the pulse switching on a wall transforms to the asymmetric Néel wall 5(c), as in Fig. 4. When the wall structure becomes similar to the classical Néel wall 5(d) the field pulse is switched off. The width  $\Delta t_2$  will be denoted by  $\Delta t_M$  that is minimal for  $\Delta t_2$  and maximal for  $\Delta t_1$ . As is seen in Fig. 5 a complicated rearrangement in the internal structure of a wall occurs, and a wall with a 5(d) structure transforms to a wall with a 5(e) structure that is also the asymmetric Néel wall, but with an opposite chirality and opposite tilt angle of the central line of

the wall. Then near the upper surface, an asymmetric vortex nucleates with a chirality opposite to the initial vortex chirality, and the wall transforms to the asymmetric Bloch wall with a vortex shifted to the upper surface 5(f). Finally, after vortex traverses the film center and shifts to the lower surface 5(g), the steady state configuration 5(h) differing from the initial 5(b) structure by chirality is established. In contrast to Fig. 4 after switching off of the field pulse a complicated relaxation of a wall structure to a new stationary state occurs that consists of a sequence of nonlinear dynamic transformations in the intrawall magnetization distribution, and, as a result, the 5(b)  $\rightarrow$  5(h) transition takes place.

**4. The nature of interwall transitions and comparison of transitions at different pulse durations**

The nature of such a great difference in the wall structure relaxation after switching-on pulses of different durations is related to the mechanism of a wall motion elucidated in Ref. 4. According to Schryer and Walker<sup>4</sup> a wall moves only after the appearance of magnetization component  $\Delta M_x$  normal to the film surface, or, in terms of one-dimensional Bloch walls, only after magnetization deviates from the film surface. These deviations at  $H > H_c$  are not stationary due to the violation of a balance of angular momentum (see Refs. 4 and 27), and the magnetization  $\mathbf{M}$  begins to precess about an easy axis. As a consequence,  $\Delta M_x$  begins to oscillate inducing the dynamic rearrangement of a wall structure (see the details in Refs. 4, 5, and 17–20). It is clear that if before the pulse termination the deviation  $\Delta M_x$  does not reach its maximal value  $(\Delta M_x)_{max}$  (always less than the saturation induction), then it relaxes to the last of the previous steady state solutions. If the field pulse is switched off after reaching  $(\Delta M_x)_{max}$  then the magnetization precession continues until

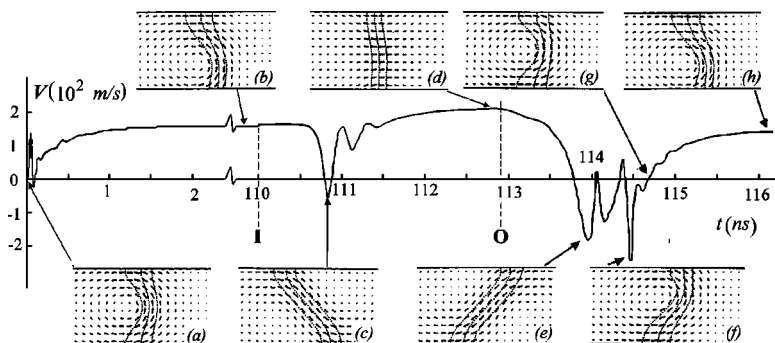


FIG. 5. The same as in Fig. 4, but pulse duration  $\Delta t=2.9$  ns.

the wall reaches the nearest stationary state. Figure 5(d) shows the magnetization configuration that corresponds to the maximal value of  $\Delta M_x$ . Note that it is not stationary. The stationary configurations are only the asymmetric Bloch walls with vortices that have unequal chiralities and are shifted to a film surface, and the asymmetric Néel walls with unequal chiralities and opposite tilt of the central line (the latter is valid only for  $H=0$ ). If  $H \neq 0$ , then the 4(c) configuration is the only stationary one, while the 4(e) configuration is not stationary for the chosen field direction ( $H \parallel z$ ). It will be stationary only with the field reversed. Thus, short field pulses can change the internal structure of domain walls. This could be applied to magnetic recording and read-out. In cases considered up to three stationary states can be obtained. The initial state of a 4(b) type that is formed after applying an external magnetic field and terminating all the transient processes where the intrawall vortex is shifted to the lower film surface and the magnetization curling (chirality) in it corresponds to the counterclockwise rotation of  $\mathbf{M}$ , and for a field pulse duration equal to  $\Delta t_1$  the wall structure transforms to a 4(d) type structure (asymmetric Néel wall). One can recognize the rearrangement of the asymmetric Bloch wall to the asymmetric Néel wall by its velocity, since the velocity of the asymmetric Néel wall is greater than the asymmetric Bloch wall velocity. The velocity difference here is only about 16%, but can be increased if the field  $H=H_1$ , for which the wall moves in a steady state before a pulse switching on, which is less than  $H=H_2$ , the field, for which the wall moves in steady state after a pulse switching off. From Fig. 5 it follows that if a pulse duration is equal to  $\Delta t_2$ , then after the pulse termination the wall becomes an asymmetric Bloch wall, but with a chirality opposite to that of the initial asymmetric Bloch wall. Two such walls can be distinguished by applying a small field  $H_x < H_a$ . In the fields  $H_x$  of opposite directions the wall vortices shift to opposite film surfaces. Given  $H_i$  and film parameters, the  $\Delta t_1$  and  $\Delta t_2$  obey the conditions  $\Delta t_m \leq \Delta t_1 \leq \Delta t_M$  and  $\Delta t_M \leq \Delta t_2 \leq \Delta t_m + T/2$ , where  $T$  is the period of a wall rearrangement in the field  $H_T = H + H_i$ . This field exceeds the critical field  $H_c$ . The above considerations imply that the quantities  $\Delta t_m$  and  $\Delta t_M$  play an important role in the transitions between different stationary

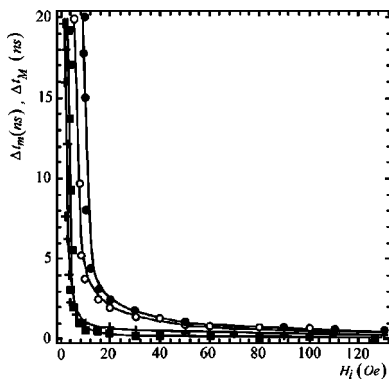


FIG. 6. Dependence of minimal pulse durations on the pulsed field. Solid circles  $-\Delta t_M$  ( $b=50$  nm). Open circles  $-\Delta t_M$  ( $b=100$  nm). Crosses  $-\Delta t_m$  ( $b=50$  nm). Solid rectangles  $-\Delta t_m$  ( $b=100$  nm). Films with basal parameters,  $\alpha=0.1$ ,  $H=90$  Oe.

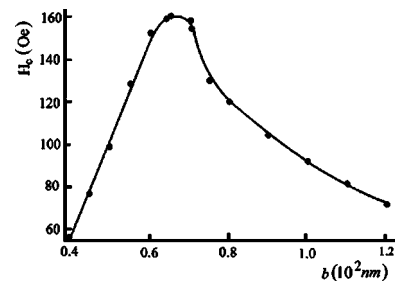


FIG. 7. Dependence of the critical field on the film thickness,  $\alpha=0.1$ .

states. Figure 6 shows that the higher  $H_i$  the shorter these times.

Such behavior results from the following. When  $H_i$  decreases, the field  $H_T$  approaches the critical field  $H_c$  from above. According to Refs. 18–20 the period required for the nonlinear dynamic rearrangement of a wall increases. As a consequence, the lifetime of intermediate wall configurations increases.

5. Interwall transitions in relatively thick films. Effect of saturation induction

The quantities  $\Delta t_m$  and  $\Delta t_M$  also strongly depend on magnetic parameters and film thickness. The character of interwall transitions induced by the pulsed field may radically change. The nature of such a behavior is related to the dependence of critical field  $H_c$  on the above mentioned parameters. In particular, as it follows from Figs. 7 and 8, the dependence of critical field on the film thickness and saturation magnetization proved to be nonmonotonic, the physical reason for which is the change of the character of dynamic rearrangement of the wall structure with  $b$  and  $M_s$  increasing.<sup>19,20</sup>

When  $b$  and  $M_s$  are increased, the (5d) configuration becomes unrealizable due to a great increase of the density of volume magnetostatic charges. The change of rearrangement character occurs for such film thickness that corresponds to the maximum of the  $H_c(b)$  curve. Hence, the transitions shown in Figs. 4 and 5 should occur in Permalloy films when  $50 \leq b \leq 65$  nm. For  $b > 65$  nm the character of the nonlinear wall dynamic rearrangement changes. The steady state wall configurations and interwall transitions induced by the

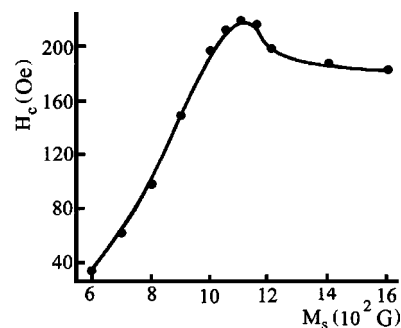


FIG. 8. Dependence of the critical field on the saturation magnetization, 50 nm thickness,  $\alpha=0.1$ .

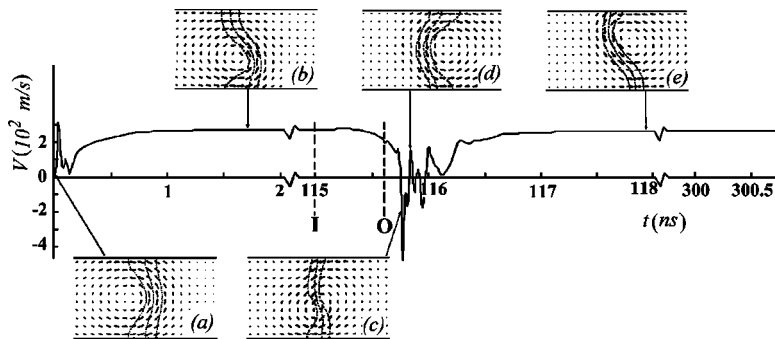


FIG. 9. Time dependence of the velocity of walls in constant field  $H=90$  Oe and pulsed field  $H_i=15$  Oe, 100 nm thickness,  $\alpha=0.1$ , pulse duration  $\Delta t=0.6$  ns. Wall configurations (a)–(e) illustrate the rearrangement of a wall during its motion. The pulse beginning and ending times are denoted in the figures by the letters **I** and **O**, respectively.

pulsed field also change. Three ranges of the field pulse duration: (1)  $\Delta t < \Delta t_{1m}$ , (2)  $\Delta t_{1m} \leq \Delta t \leq \Delta t_{1M}$ , and (3)  $\Delta t_{1M} \leq \Delta t \leq \Delta t_{1m} + T/2$  are possible in this case.  $\Delta t_{1m}$  is the minimal pulse duration, with which the rearrangement of an initial steady state of a 3a type begins.  $\Delta t_{1M}$  is the minimal pulse duration, at which an initial steady state of a 3c type begins to decay. And again, for pulse durations from the first range  $\Delta t < \Delta t_{1m}$  a wall relaxes to the initial state. More interestingly cases (2) and (3) will be called the short and long intervals. Figures 9 and 10 show the transitions for the films 100 nm thick and the same other parameters as in Figs. 4 and 5.

Pulse durations  $\Delta t_1$  and  $\Delta t_2$  correspond to the short and long intervals. The  $\Delta t_{1m}$  is a minimal pulse duration, from which the rearrangement  $9(b) \rightarrow 9(c)$  begins, and the  $\Delta t_{1M}$  is a minimal pulse duration required for beginning the  $10(e) \rightarrow 10(f)$  rearrangement. A wall velocity decreasing can reveal the onset of such a rearrangement.

Thus, two different types of dynamic wall rearrangement exist depending on what duration of a pulse is chosen. The existence of two pulse duration intervals is caused by the same physical reasons considered above for explaining the interwall transitions in relatively thin films (of thickness less than 65 nm). The character of transition in the films with  $b=100$  nm and  $b=50$  nm is different in spite of the same mechanisms inducing the interwall transitions. Let us consider these transitions in detail.

#### 6. Interwall transitions for the short interval of pulse durations

If at  $t=115$  ns, when the stationary state configuration is (b) (Figs. 9 and 10), a pulse of a  $\sim 0.6$  ns duration and an amplitude of  $H_i=15$  Oe is triggered, it induces the (b)  $\rightarrow$  (c) rearrangement. Despite the fact that after some decreasing of the wall velocity the pulse action terminates, the

structure and velocity of the wall do not relax to the previous state. Instead, the wall structure continues to rearrange in a complicated way passing a whole sequence of instantaneous configurations. Two of them (c) and (d) are shown in Fig. 9. Finally, a new stationary state 9(e) is established similar to the 3(c) state, but differs from the latter by that it is obtained from one and the same left-asymmetric 9(a) configuration along with the 9(b) configuration. At the same time, the 3(c) configuration is obtained from the right-asymmetric 2(c) configuration by applying a constant field of the same value and direction (along the  $z$  axis) as the configuration in Fig. 3(a). Thus, the pulse of the  $\Delta t_1$  duration induces a  $9(b) \rightarrow 9(e)$  transition from a wall with a left-asymmetric configuration whose vortex center is shifted to the lower surface to a wall with a right-asymmetric configuration whose vortex center is shifted to the upper surface. Using such pulses, we were unable to obtain the asymmetric Néel structure for the thicknesses we examined.

#### 7. Interwall transitions for the long interval of pulse durations

The situation substantially differs, if after an establishment of the stationary motion [with a 10(b)-type structure], a pulse with an amplitude  $H_i=15$  Oe and  $\Delta t_2=2.3$  ns duration is applied. In this case, under the action of a pulse (see Fig. 10) a wall acquires the 10(e) configuration after a sequence of transformations. If after the onset of a rearrangement of this state the action of a pulse ceases, nevertheless the rearrangement goes on and [via an intermediate configuration of a 10(f) type] a wall transforms to a stationary state 10(g), that only differs from the initial stationary state 10(b) by a chirality. Such stationary states can be distinguished, for example, by applying a small field (less than  $H_a$ ) directed along the  $x$  axis. Both the vortices will shift in opposite directions

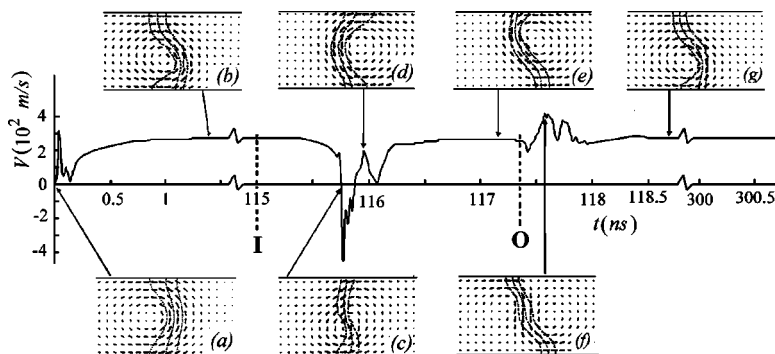


FIG. 10. The same as in Fig. 9, but pulse duration  $\Delta t=2.3$  ns.

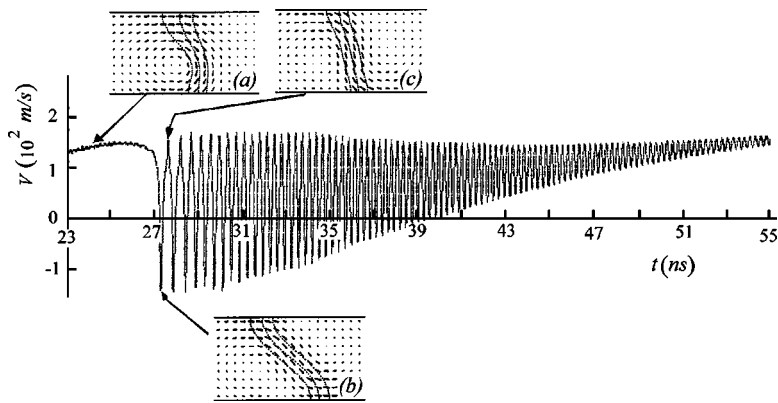


FIG. 11. Time dependence of the velocity of walls in constant field  $H=1.7$  Oe and pulsed field  $H_i=2.3$  Oe, 100 nm thickness,  $\alpha=0.001$ , pulse duration  $\Delta t=3.8$  ns. Wall configurations (a)–(c) illustrate the rearrangement of a wall during its motion.

in such a field. Note that stationary state 10(g) agrees in shape with that found in Ref. 28 by the Ritz method and for the other situation, namely, for an inertial motion of a wall, but we consider the forced motion of a wall under the action of a pulsed magnetic field.

In the films 100 nm thick the magnitudes  $\Delta t_{1m}$  and  $\Delta t_{1M}$  also depend on  $H_i$  (see Fig. 6) and this dependence is the same as in the films with 50 nm thickness. Moreover, we believe that it is valid in a wider range of film thickness according to the above considerations.

**8. Interwall transitions for different values of induction**

Similar conclusions can be drawn for the case of the saturation induction  $B_s=4\pi M_s$  varying. The situation in Figs. 4 and 5 corresponds to  $B_s \in [0.5-1.4]$  T. If  $B_s > 1.4$  T, then the rearrangement of a wall structure similar to that shown in Figs. 9 and 10 occurs.

**9. Interwall transitions for different values of damping**

The above numerical computations were carried out for the damping  $\alpha=0.1$ , and we also studied the processes in the films with  $\alpha \in [0.1-0.001]$ . The  $\alpha$  decreasing does not lead to any new wall transitions, but during the establishment of the stationary states before and after the pulse action at small damping (for example, at  $\alpha=0.001$ ) quite long oscillations of a velocity appear, the nature of which was revealed earlier.<sup>18</sup>

Figures 11 and 12 show, as an example, the transitions for  $\alpha=0.001$ , and the stationary states 11(a) and 12(a) are established in the  $H=1.7$  Oe field.

Such a small propulsive field is chosen since at small  $\alpha$  the critical field proves to be also small (of  $\sim 2.2$  Oe). It should be reminded that for establishing a steady state without a pulsed field the condition  $H < H_c$  should be fulfilled. If a pulse has 3.8 ns duration and  $H_i=2.3$  Oe amplitude, then after its switching-off (see a point **O**) and long subperiodic oscillations (see Ref. 18) a change of the span of the wall central line occurs [compare configurations Fig. 11(b) and Fig. 11(c)] and the stationary state establishes that it is an asymmetric Néel wall with an intermediate between 11(b) and 11(c) span of the central line. It should be reminded that subperiodic oscillations mean the changes of a wall velocity within a period of dynamic transformations of a wall structure.<sup>18</sup> The oscillations always appear when the internal magnetostatic fields sharply change upon the wall rearrangement.

If under the same conditions a pulse duration is equal to 20 ns, then, as it follows from Fig. 12, after a sequence of transformations similar to Fig. 10 and accompanied by subperiodic oscillations a new stationary state 12(e) is established that is similar to the initial 12(a) state, but with the opposite chirality. Thus, the subperiodic oscillations that appear at small  $\alpha$  do not change the character of the transitions induced by the pulsed magnetic field. The pulse duration, at which the transitions shown in Figs. 11 and 12 occur, also

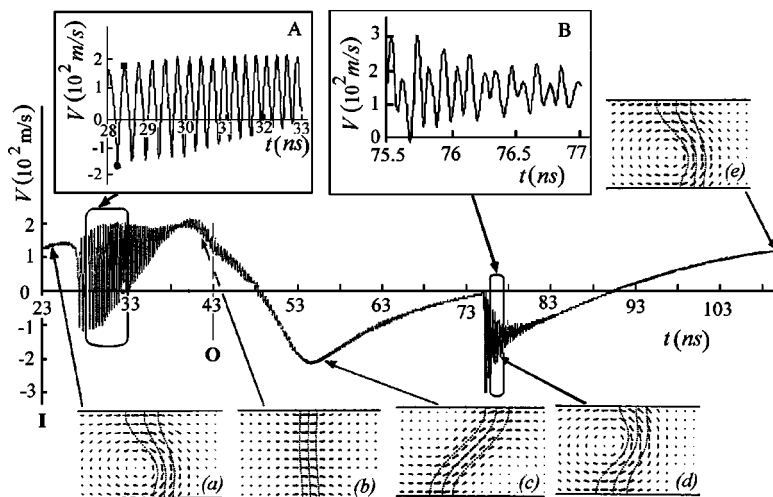


FIG. 12. The same as in Fig. 11, but pulse duration  $\Delta t=20$  ns. The pulse beginning and ending times are denoted in the figures by the letters **I** and **O**, respectively. The inserts A and B show the velocity oscillations in narrow time intervals.

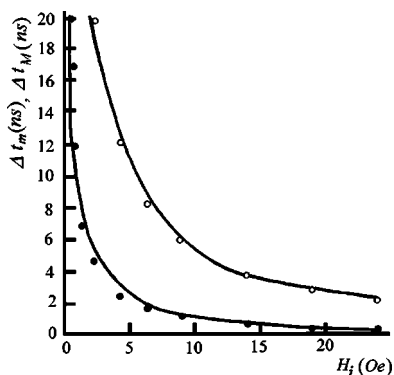


FIG. 13. Dependence of minimal pulse durations  $\Delta t_m$  (solid circles),  $\Delta t_M$  (open circles) on pulsed field for films 100 nm thick in constant field  $H=1.7$  Oe,  $\alpha=0.001$ .

depends on  $H_i$ , but according to Fig. 13 this dependence is not as sharp as at great damping.

Thus, two intervals of pulse duration appear in a wide range of the film parameters, and within these intervals various transitions between stationary states of walls can be realized.

### C. Nonlinear dynamics of walls in periodic pulse fields

#### 1. The influence of periodically repeated field pulses on dynamic rearrangements of wall structure

As was noted above (see Sec. III A), if  $H \geq H_c$ , then in a constant field the wall velocity and its internal structure vary periodically. In particular, in the films with basal parameters  $b=50$  nm thick with  $\alpha=0.1$  and at  $H \in [100-150]$  Oe the sequence of wall structure rearrangements  $(a) \rightarrow (b) \rightarrow (c) \rightarrow (d) \rightarrow (e) \rightarrow (f) \rightarrow (g)$  is similar to that shown in Fig. 5. However, in contrast to Fig. 5, corresponding to a pulsed field, this sequence occurs during a period of wall velocity changes. It is important that although the states  $(a)$  and  $(g)$  are alike, they differ in chirality. During the next period the sequence is analogous, but at the very end the wall structure comes back to the initial  $(a)$ . Thus, degeneracy over chirality of the wall periodic motion velocity takes place in a constant magnetic field. The character of nonlinear dynamic rearrangement substantially depends on different magnetic parameters of a film and its thickness.<sup>5,18-20</sup>

The studies performed and the data obtained earlier<sup>18-20</sup> show that the period  $T$  of the wall dynamic rearrangements is mainly determined by the lifetime of some wall configurations [for example, of a  $5(c)$ ]. Such determining configurations are different for the films with different parameters. For example, in the films with basal parameters and  $b=100$  nm thick the  $9(e)$  is a determining configuration. The existence of determining configurations suggests an idea to control the period of intrawall dynamic rearrangement applying magnetic field pulses of a relatively short duration  $\Delta t < T$  at certain time instants. Moreover, it is possible with such pulses to obtain periodic rearrangements in the internal wall structure in the fields lower than  $H_c$ , which gives additional possibilities of controlling the wall velocity without changing

the film parameters. We give below some examples of controlling the dynamic rearrangement in the wall internal structure and its velocity period by triggering the periodically repeated pulses with various amplitude and duration. With the above assumption  $H+H_i > H_c$  and  $H_i < H_c$ , the periodic dynamic rearrangement in the wall internal structure and periodic changes of its velocity can only be attained by synchronizing the switching on of a pulse with the instant appearance of the determining configuration. If  $H_i > H_c$  and the pulse duration is sufficiently high, then periodic dynamic rearrangement in the wall internal structure can be attained without any synchronization.

#### 2. Inducing the wall structure periodic dynamic rearrangements at $H_i < H_c$

Our studies show that in uniaxial films inducing the periodic dynamic rearrangement in the wall internal structure and periodic changes of its velocity can be realized in a wide range of thickness and magnetic parameters. The appearing effects are qualitatively similar in all the cases, and slight variations are only related to the particular character of dynamic rearrangement in the particular cases, which will be shown in some examples.

Consider films with basal parameters  $b=100$  nm thick and with  $\alpha=0.001$ . In such films the critical field is  $H \approx 1.3$  Oe. If in this case  $H=1$  Oe and  $H_i=0$ , then after termination of the transient process (of about 120 ns) the stationary wall motion with the configuration shown in Fig. 14(c) (upper solid curve) and the velocity  $\approx 230$  m/s is established.

In this case, the constant external field is insufficient for inducing the rearrangement of a  $14(c)$  state, but triggering the  $H_i=0.5$  Oe pulsed field substantially changes the situation. Since here  $H_i$  is low enough ( $H_i < H_c$ ), it is necessary to synchronize the pulse switching on and the instant of a  $14(c)$ -type structure formation in order to obtain the periodic rearrangements in the internal structure of a wall and its velocity. If in addition to the  $H$  field at the instants, when a  $14(c)$ -type structure appears, one switch on the pulses with an amplitude  $H_i=0.5$  Oe and  $\Delta t_i=60$  ns duration and switch them off at the instants, when the structure of  $14(d)$  type appears, then the behavior of a wall velocity actually becomes periodic with the  $T$  period of about 120 ns. Figure 14 (lower part) shows only three fragments, but it will be more obvious if one mentally translates two last fragments to the right. The periodic changes in a wall velocity are related to the periodic transformations in the internal wall structure  $b \rightarrow c \rightarrow d$ , etc. The  $T$  period decreases with increasing an amplitude of a pulsed field and with increasing a relative width of a pulse  $\Delta \theta = (\Delta t)_i / (\Delta t)_p$ , where  $(\Delta t)_i$  is a pulse duration and  $(\Delta t)_p$  is the pulse period.

#### 3. Nonlinear rearrangements of the wall structure by periodic pulses $H_i > H_c$

The considered situation required strict synchronization of switching on the pulses and the appearance of definite configurations, that makes difficulties for the experimental studies, but no synchronization is required for  $H_i > H_c$ . In this case, a very interesting situation appears. First of all, al-

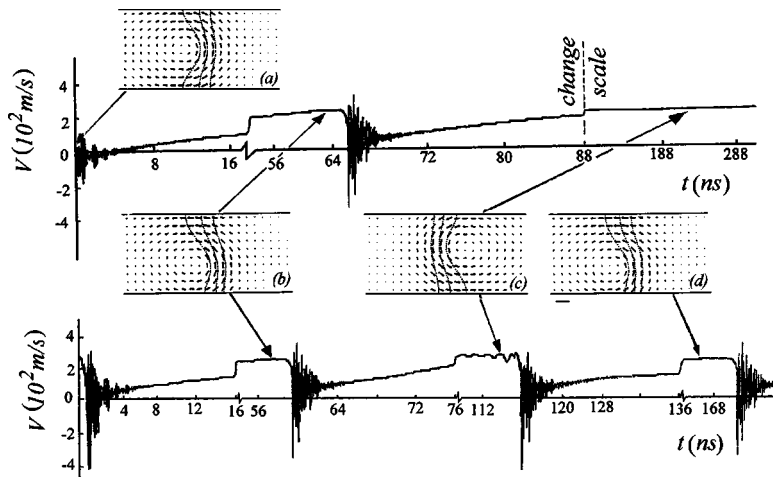


FIG. 14. Time dependence of the velocities of walls (the upper solid curve in the absence of a pulsed field, the lower curve in the pulsed field  $H_i=0.5$  Oe) and instantaneous wall configurations in constant field  $H=1.0$  Oe, 100 nm thickness,  $\alpha=0.001$ .

though at some time instants an external field does not influence the wall, the nonlinear rearrangements in the wall internal structure undergo the same sequences as in the presence of a constant external field. Moreover, beginning with some configuration the system comes back to the same configuration in some time. Figure 15 shows one of the examples, in which small  $\alpha$  is chosen to show all the peculiarities of the wall structure dynamic rearrangements in a pulsed field, the subperiodic oscillations included.

We included in the figure the instantaneous wall configurations to illustrate its structure in the maxima and minima of subperiodic oscillations. Let us call the time, upon which the initial wall configuration after a sequence of transformations comes back to the initial state, a quasiperiod and denote it by  $T_c$ . In spite of an astonishing similarity between the wall nonlinear dynamic rearrangements in a constant and pulsed field, the velocity behaves differently in successive portions of  $T_c$ . Moreover, the successive values of the quasiperiod vary at random, which is related to the incommensurability of the period of the wall dynamic rearrangements in a given field and a period of pulse succession. Figure 16 shows, as an example, five successive time intervals, corresponding to different values of  $H_c$ .

In each row of the figure, a change in the velocity averaged over the film thickness is brought out under the condition that the initial and final graph points strictly correspond to one and the same instantaneous wall structure. The quasiperiods at the successive time intervals are seen to vary at

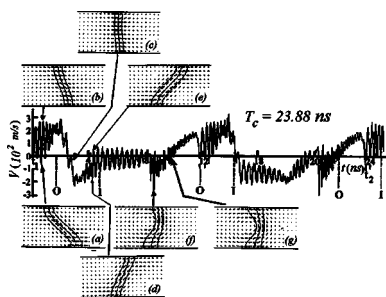


FIG. 15. Time dependence of the velocity of walls (solid curves) and instantaneous wall configurations in constant field  $H=20$  Oe and pulsed field  $H_i=0.5$  Oe, 50 nm thickness,  $\alpha=0.001$ .

random. In the present case (the  $H_i$  field is great in comparison to  $H_c$ ) these changes are not great (of about 15%), but they increase with  $H_i$  approaching  $H_c$ .

Thus, in order that the process be close to a periodic one it is necessary for the magnitude of  $H_i$  to substantially differ from  $H_c$  and to be more the less is the magnitude of  $\Delta\theta$ . It is better for the magnitude of  $(\Delta t)_p$  to be less or on the order of  $T$  in the field  $H$  of the same value as  $H_i$ . In such a situation, the change in the period of an almost periodic process of nonlinear intrawall rearrangement will be observed with the  $(\Delta t)_p$  variation. Figure 17 shows the variation of a quasiperiod (averaged over a great number of them) of wall dynamic rearrangements in the field  $H_i=20$  Oe and with a frequency  $1/(\Delta t)_p=5 \times 10^{-9} \text{ s}^{-1}$  in the films with basal parameters and  $\alpha=0.001$ .

Varying the pulse duration, one can diminish (augment) the period of a wall dynamic rearrangement. Hence, using

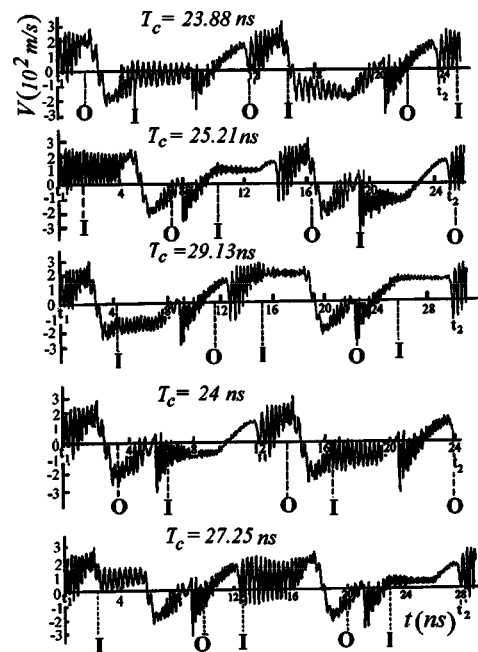


FIG. 16. The quasiperiod variation upon domain wall motion in constant field  $H=20$  Oe and pulsed field  $H_i=0.5$  Oe, 50 nm thickness,  $\alpha=0.001$ .

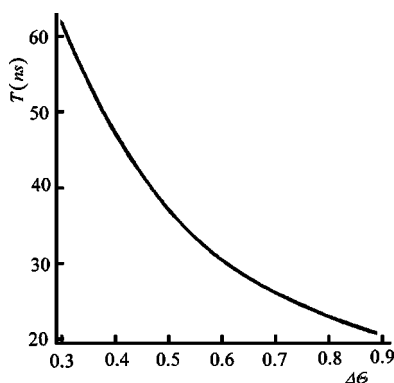


FIG. 17. Dependence of the quasiperiod of domain wall dynamic rearrangements on the relative pulse duration in constant field  $H=20$  Oe. The pulse recurrence frequency is  $5.0 \times 10^9$  Hz.

the pulsed fields one can vary the velocity of a domain wall translational motion. Switching on the pulsed fields at certain time instants one can inhibit the wall dynamic rearrangement, and, as a consequence, increase the maximal velocity of their translational motion.

#### IV. EXPERIMENTAL POSSIBILITIES FOR OBSERVATION OF PREDICTED EFFECTS

The asymmetric walls of Bloch and Néel types were observed in a series of papers<sup>12–16</sup> with high-voltage electron microscopes. The magnetization profiles in a specific direction were obtained by scanning a film along its surface in the direction normal to the wall plane and compared with the calculated profiles (see, for example, Refs. 14–16). The thus obtained data support the existence of the asymmetric walls as real entities.

Although the considered transitions  $4(b) \rightarrow 4(d)$  and  $5(b) \rightarrow 5(h)$  occur in the external field, similar transitions can also occur at  $H=0$ . The latter case is the most favorable for experimental observation of these interwall transitions, since it allows studying the structures of final states by the same electron microscopic methods as in Refs. 12–14. All the states of  $4(b)$ ,  $5(b)$ , and  $5(h)$  types will have unshifted vortices, but it is important that chiralities of  $5(b)$  and  $5(h)$  states are opposite. In this case, the profiles  $\overline{M}_y(x)$  (here an overbar means the averaging over the film thickness) of these states will be different. For the sake of convincingsness the bias field (less than the anisotropy field) can be applied along the  $x$  axis. Such a field shifts the vortices with opposite chiralities to different surfaces resulting in different distortions of the magnetization profiles that could be observed with an electron microscope. The other transitions could be studied similarly.

The films with the least possible damping should be taken to decrease the pulsed field amplitude, as it follows from the above considerations. Thus, at  $\alpha=0.001$  the amplitude can be on the order of 1 Oe. Note also that although the basal parameters chosen for computations correspond to Permalloy films the results obtained are valid for other films with quality factor  $Q < 1$ . Another method for choosing reasonable pulsed field amplitudes avoiding films with extremely low

damping is the investigation of transitions in a nonzero external field, as in computations, but  $H$  should be put to zero in the final state. In this case the vortices will shift to the film center, but the chirality and the direction of the wall central line bending will be retained that will affect the magnetization profiles and could be observed with an electron microscope.

#### V. CONCLUSIONS

The numerical simulation of the nonlinear dynamic behavior of two-dimensional asymmetric vortexlike domain walls predicts the existence of the critical field  $H_c$ , above which wall motion is nonstationary in a constant magnetic field. The existence of various steady state configurations are caused by isolated magnetic field pulses added to the background of the propulsive magnetic field. Transitions between different stationary states can occur, and various states can exist at a given propulsive field, which do not occur without pulses. Two different intervals of pulse duration exist, in which the character of dynamic rearrangement in the internal wall structure leads to quite different final steady state solutions. The intervals are narrower as the strength of the magnetic field pulse increases. Making use of the periodicity in the changes of a wall structure and velocity, the intervals mentioned could be shifted along the time axis, thus creating opportunities for experiments.

The transitions between stationary states are possible in the films both with a small ( $\alpha=0.001$ ) and great ( $\alpha=0.1$ ) damping, and the transition process (appearing intermediate configurations of the magnetization) at a small damping is virtually independent of damping. All the states at a small damping are accompanied by subperiodic vibrations of some parts of the walls relative to the other parts, which develop due to the fast changes of inhomogeneous magnetostatic fields induced by the transitions between some wall configurations. Despite the similar behavior of dynamic rearrangements at a small and great damping the evident advantage belongs to the films with a small damping, since it allows applying pulses of low amplitudes.

Moreover, the dependence of the intervals of pulse duration, in which the transitions occur, on the  $H_i$  magnitude proves to be smoother, and the very intervals more wider than in the films with a great damping. Drastic changes in the character of the nonlinear transition between different stationary states happen either with changes in the film thickness or the magnitude of the saturation induction. In this case, both the stationary states and intermediate instantaneous wall configurations, via which the transition occurs, are changed. The transition changes with a film thickness or the saturation induction have the same nature as do the critical field changes. These changes are caused by the impossibility of the existence of some configurations because of the high magnetostatic fields of such configurations.

In the presence of periodic successive pulses one can obtain the same dynamic wall rearrangements as in constant fields. If in this case the switching-on of periodic successive pulses is tied to the onset of a definite wall configuration, then one can obtain the periodic transformations of a domain

wall structure in propulsive fields lower than the critical one. Without such a tie, periodic successive pulses with amplitude higher than the critical field lead to the same rearrangements in the internal wall structure (with the very same instantaneous configurations) as the constant magnetic field above the critical one.

For a given structure, and within the  $T_c$  (a quasiperiod) time interval the internal structure of a wall returns to the fixed one after a sequence of substantial nonlinear transformations. However, the quasiperiod varies with time in a random way, which is related to the incommensurability of the period of pulse application with the period of dynamic rear-

rangements in the internal wall structure under the action of the constant magnetic field equal to the amplitude value of the pulsed field. The studies have shown that varying a pulse duration can change the period of the wall transformations and the period of its oscillations. Thus, making use of the pulsed magnetic field one can control the velocity of the wall translational motion arbitrarily.

#### ACKNOWLEDGMENT

This work was partly supported by the Russian Foundation for Basic Research, Project No. 02-02-16443.

- 
- <sup>1</sup>A.P. Malozemoff and J.C. Slonczewski, *Magnetic Domain Walls in Bubble Materials* (Academic, New York, 1979).
- <sup>2</sup>A. Hubert, *Theorie der Domänenwänden in Geordneten Medien* (Springer-Verlag, New York, 1974).
- <sup>3</sup>F. Bloch, *Z. Phys.* **74**, 295 (1932).
- <sup>4</sup>N. L. Schryer and L. R. Walker, *J. Appl. Phys.* **45**, 5406 (1974).
- <sup>5</sup>S. W. Yuan and H. N. Bertram, *Phys. Rev. B* **44**, 12395 (1991).
- <sup>6</sup>B. Petek, P. L. Trouilloud, and B. E. Argyle, *IEEE Trans. Magn.* **26**, 1328 (1990).
- <sup>7</sup>N. X. Sun and S. X. Wang, *IEEE Trans. Magn.* **36**, 2506 (2000).
- <sup>8</sup>N. Ouama, T. Ruwashima, O. Matsuda *et al.*, *IEEE Trans. Magn.* **36**, 2509 (2000).
- <sup>9</sup>A. E. LaBonte, *J. Appl. Phys.* **40**, 2450 (1969).
- <sup>10</sup>A. Hubert, *Phys. Status Solidi* **32**, 519 (1969).
- <sup>11</sup>B. N. Filippov and L. G. Korzunin, *IEEE Trans. Magn.* **29**, 2563 (1993).
- <sup>12</sup>S. Tsukahara and H. Kavakatsu, *J. Phys. Soc. Jpn.* **32**, 1993 (1972).
- <sup>13</sup>T. Suzuki, K. Suzuki, and I. Igorashi, *Jpn. J. Appl. Phys.* **15**, 707 (1976).
- <sup>14</sup>J. N. Chapman, G. R. Morrison, and J. P. Jakubovics, *J. Magn. Mater.* **49**, 277 (1985).
- <sup>15</sup>M. R. Scheinfein, J. Unguris, R. J. Celotta *et al.*, *Phys. Rev. Lett.* **63**, 668 (1989).
- <sup>16</sup>M. R. Scheinfein, J. Unguris, J. L. Blue *et al.*, *Phys. Rev. B* **43**, 3395 (1991).
- <sup>17</sup>B. N. Filippov and L. G. Korzunin, *Phys. Met. Metallogr.* **95**, 427 (2003).
- <sup>18</sup>B. N. Filippov, L. G. Korzunin, and F. A. Kassan-Ogly, *Phys. Rev. B* **64**, 104412 (2001).
- <sup>19</sup>B. N. Filippov, L. G. Korzunin, and F. A. Kassan-Ogly, *Solid State Commun.* **121**, 55 (2002).
- <sup>20</sup>B. N. Filippov and L. G. Korzunin, *Zh. Eksp. Teor. Fiz.* **94**, 315 (2002).
- <sup>21</sup>A. Aharoni, *J. Appl. Phys.* **39**, 861 (1968).
- <sup>22</sup>M. LaBrune and J. Miltat, *J. Appl. Phys.* **75**, 2156 (1994).
- <sup>23</sup>L. I. Antonov, E. V. Lukasheva, and E. A. Mukhina, *Phys. Met. Metallogr.* **80**, 312 (1995).
- <sup>24</sup>L. D. Landau and E. M. Lifshitz, *Phys. Z. Sowjetunion* **8**, 153 (1935).
- <sup>25</sup>G. I. Marchuk, *Methods of Calculus Mathematics* (Nauka, Moscow, 1989).
- <sup>26</sup>A. A. Thiele, *J. Appl. Phys.* **45**, 377 (1974).
- <sup>27</sup>B. N. Filippov and A. P. Tankeev, *Dynamical Effects in Ferromagnets with Domain Structure* (Nauka, Moscow, 1987).
- <sup>28</sup>A. Aharoni and J. P. Jakubovics, *IEEE Trans. Magn.* **26**, 2810 (1990).